

# **Electric Field Induced in Retina and Brain at Threshold Magnetic Flux Density Causing Magnetophosphenes**

Akimasa Hirata<sup>1</sup>, Yukinori Takano<sup>1</sup>, Osamu Fujiwara<sup>1</sup>, Thanh Dovan<sup>2</sup>, and Robert Kavet<sup>3</sup>

1: Nagoya Institute of Technology, Department of Computer Science and Engineering, Japan

2: SP AusNet, Division of Network Strategy & Development, Australia

3: Electric Power Research Institute, Palo Alto, CA USA

## Abstract

For magnetic field exposures at extremely low frequencies, the electrostimulatory response with the lowest threshold is the magnetophosphene, a response that corresponds to an adult exposed to a 20-Hz magnetic field of nominally 8.14 mT. In the IEEE standard (2002) the corresponding *in-situ* field in the retinal locus of an adult-sized ellipsoidal was calculated to be 53 mV/m. However, the associated dose in the retina and brain at a high level of resolution in anatomically-correct human models are incompletely characterized. Furthermore, the dose maxima in tissue computed with voxel human models are prone to staircasing errors, particularly for the low-frequency dosimetry. In the analyses presented in this paper, analytical and quasi-static FDTD solutions were first compared for a three-layer sphere exposed to a uniform 50-Hz magnetic field. Staircasing errors in the FDTD results were observed at the tissue interface, and were greatest at the skin-air boundary. The 99<sup>th</sup> percentile value was within 3% of the analytic maximum, depending on model resolution, and thus may be considered a close approximation of the analytic maximum. For the adult anatomical model, TARO, exposed to a uniform magnetic field, the differences in the 99<sup>th</sup> percentile value of *in-situ* electric fields for 2-mm and 1-mm voxel models were at most several percents. For various human models exposed at the magnetophosphene threshold at three orthogonal field orientations, the *in-situ* electric field in the brain was between 10% and 70% greater than the analytical IEEE threshold of 53 mV/m, and in the retina was lower by roughly 50% for two horizontal orientations (anterior-posterior and lateral), and greater by about 15% for a vertically-oriented field. Considering a reduction factor or safety factors of several fold applied to electrostimulatory thresholds, the 99<sup>th</sup> percentile dose to a tissue calculated with voxel human models may be used as an estimate of the tissue's maximum dose.

## 1. Introduction

There has been increasing public concern regarding potential health effects associated with electromagnetic fields. Safety guidelines/standards for electromagnetic field exposures have been established by different organizations (ICNIRP 1998, IEEE 2002, ICNIRP 2010) with the objective of protecting people against electrostimulation, the only potentially adverse effect established for extremely-low-frequency exposure. In the frequency range up to several hundred hertz, the lowest *in-situ* electric field threshold electrostimulation response is the production of magnetophosphenes, a response mediated in the retina. Note that the retina is part of the central nervous system (CNS) and is regarded as an appropriate model for induced electric field effects on CNS neuronal circuitry in general (IEEE 2002, ICNIRP 2010). The IEEE standard (2002) expresses the basic restriction in terms of the *in-situ* electric field averaged over a 5 mm-long straight-line segment of tissue. The latest ICNIRP guideline (2010) uses *in-situ* electric field averaged over a 2-mm cube replacing the previous dosimetric basis of induced current density averaged over 1 cm<sup>2</sup> (1998). Even though different averaging procedures for *in-situ* electric field are applied by IEEE and ICNIRP, their rationale is almost identical (Reilly 1998). To assign a maximum dosimetric quantity in tissue, the ICNIRP (2010) applies the 99<sup>th</sup> percentile value due to major uncertainties concerning the true maximum value. The 99<sup>th</sup> percentile value was first applied to an anatomically-based model by Hirata *et al* (2001) based on the computational investigation of Dawson *et al* (2001). The maximum induced electric field/current density may include computational errors attributed to the staircasing approximation of the model, which is particularly evident at low frequencies. The model used in that investigation was a homogeneous, two-layer sphere with inner and outer diameters of 1.10 mm and 1.20 mm, respectively, with resolutions of either 3.6 mm or 7.2 mm (Dawson *et al* 2001). When considering magnetophosphenes and the dose metrics used in recent international

standard/guidelines (IEEE 2002, ICNIRP 2010), a model with higher resolution would be advisable, especially for a tissue with small numbers of voxels, such as the retina.

In the present study, the effect of model resolution on the *in-situ* electric field induced by a 50 Hz magnetic field is investigated with a three-layer sphere comprised of skin, skull and brain. Then, the statistical characteristics of the *in-situ* electric field are presented to provide a basis for introducing the 99<sup>th</sup> percentile value as a practical estimate of the maximum induced field in a given anatomical site. Based on these findings, we calculated the electric fields induced in the brain and retina of different human models exposed to a magnetic field at the most sensitive frequency and threshold reported for producing magnetophosphenes (Lovsund et al 1980).

## **2. Model and Methods**

### **2.1. Multi-layer Sphere and Physical Human Models**

The radius of the multi-layer sphere is 100 mm and comprised of three tissues; the skin, skull, and brain. The thicknesses of the skin and skull are 2 mm and 8 mm, respectively. The electrical constants of the skin, skull, and brain are 0.1, 0.02, and 0.1 S/m, respectively.

In order to discuss the variability of *in-situ* electric field in different anatomical human numeric models, seven were considered, including the Japanese male and female models named TARO and HANAKO, respectively, (Nagaoka *et al* 2004) and a three-year-old child model developed from TARO (Nagaoka *et al* 2008). All of these models are segmented into 51 anatomic regions. In addition, a European male model named Duke, a female model named Ella and a six year-old male child, Thelonious, were also used (Christ *et al*, 2010). These models are comprised of 84 tissues. Another well-characterized European male model, named NORMAN consisting of 37 tissue types was also included (Dimbylow, 1997). The original resolution of each model is 2 mm. The height, weight, and the number of tissues for these models are

summarized in Table 1.

TARO was used to examine the effect of model resolution on *in-situ* electric fields. In addition to the original 2-mm resolution model, a 1-mm resolution model was created by scaling down to 1 mm by subdividing each 2-mm cell of TARO into eight 1-mm cells. Similarly to the original TARO model, manual editing was also applied to the 1-mm resolution model, with particular attention to the retina, by a medical specialist to obtain anatomical accuracy, (Hirata *et al* 2007).

## **2.2. Computational Methods**

A quasi-static finite-difference time-domain (FDTD) method (De Moerloose *et al* 1997) was used to compute the induced fields in the Japanese models. This method extends a conventional FDTD method (Taflove and Hagness 2005) to solve quasi-static problems by choosing incident waveforms appropriately. Under the quasi-static approximation, fields exterior to the conductors have the same phase as the incident field. The interior fields, on the other hand, are first-order fields that are proportional to the time derivative of the incident field. The incident field is then chosen as a ramp function with a smooth start (De Moerloose *et al.* 1997). The cell resolution was chosen as 2 mm so as to coincide with the voxel resolution of the human phantoms.

In order to generate a proper uniform magnetic, two plane waves in opposite directions were excited so that electric fields of the plane waves cancel each other. The computational region is truncated by perfectly matched layers. The tissue conductivities chosen were based on Gabriel *et al.* (1996), as summarized in our previous study (Hirata *et al* 2009). In addition, the conductivity of the retina was assigned as 0.5 S/m (Dimbylow 2005). Our computational code has been validated via an intercomparison of laboratories and codes (Hirata *et al.* 2010a).

The multi-layer sphere and human models were all assumed to be located in free space. For

the human models, three orientations of magnetic fields were considered: AP (front-to-back), TOP (top-to-bottom), and LAT (side-to-side). All models were exposed to a 1 mT, 50 Hz magnetic field, except for the model run at the magnetospheric threshold.

### 3. Computational Results

#### 3.1. Comparison of analytic and FDTD-derived Electric Fields in Three-layer Sphere

For a 1-mT, 50-Hz exposure, Figure 1 illustrates (a) the FDTD-calculated electric field in the three-layer sphere of 2-mm resolution and (b) its error relative to an analytic solution. Note that the analytic solution of induced electric field is given by Faraday's law:

$$E = \omega B r / 2 \quad (1)$$

where  $\omega$ ,  $B$ , and  $r$  denote the angular frequency and magnetic flux density of magnetic field and the distance from the center of the sphere, respectively. As seen from Fig. 1 (b), obvious differences between the analytic and FDTD-derived values of the electric field appear at the boundaries between tissues and between skin and air. In particular, the maximal error caused by the staircasing approximation was 35% and appears at the model's surface.

Figure 2 shows the FDTD and analytic percentile values of *in-situ* electric field of different tissues for the multi-layer sphere with the resolution of 0.5, 1.0, and 2.0 mm. The results are also summarized in Table 2. As seen from Fig. 2 and Table 2, the errors in maximal *in-situ* electric field computed with the FDTD method become larger with finer model resolution for skin (18.4 to 26.5%) and brain (12.9 to 15.8%). In addition, a computational model with a finer resolution provides results that agree well with analytical solution even for higher percentile values such as 99<sup>th</sup>, especially for the skin. The point to be stressed here is that the 99th percentile value of *in-situ* electric field in the skin and bone of voxel models is 1.9 to 9.2% larger or conservative compared to that of analytic maximum. For the brain, the 99th percentile

value was 2.1 to 2.8% smaller than the analytical maximum, because the volume of the brain is relatively large. For the finest resolution, the 99.8<sup>th</sup> percentile is an accurate estimate of the analytical maximum (Figure 2 (c)); for the lower resolutions, the 99.5<sup>th</sup> to 99.7<sup>th</sup> percentile provide an accurate estimate (Figures 2 (a) and (b)).

### **3.2. *In-situ* electric field in Retina and Brain of Anatomically-Based Model with Different Resolution**

For TARO, the effect of model resolution (1 mm compared to 2 mm) on the *in-situ* electric field was examined. Note that these models are not identical since a smoothing algorithm was applied to generate the high-resolution model, plus as noted earlier, manual editing was applied to the retina by a medical specialist (Hirata *et al* 2007). Figure 3 shows the percentile values of the *in-situ* electric field of the brain with resolutions of 1 mm and 2 mm. Table 3 lists the maximum, 99<sup>th</sup> percentile, and average values of the *in-situ* electric field for both resolutions. As shown in Fig. 3, the ratio of the maximum to the 99<sup>th</sup> percentile value in the anatomically-based model was 2.7 to 3.5 for 1-mm resolution, and between 2.3 and 2.8 for 2-mm resolution, which are much larger than the ratios of the analytical maximum to the computed 99<sup>th</sup> percentiles in the three-sphere model (see also Hirata *et al* 2010b). The differences of the 99<sup>th</sup> percentile values due to different model resolutions were marginal. Specifically, when normalized to the *in-situ* electric field with the resolution of 1 mm, the maximum differences of the *in-situ* electric fields between 1 mm and 2 mm resolution models were 4.9% for brain (TOP), 7.4% for retina (AP), and 8.3% for spinal cord (AP).

### **3.3. Uncertainty of *In-situ* Electric Field Caused by Tissue Conductivity**

Recently, uncertainty of tissue conductivity has been reviewed by Gabriel *et al* (2009). In order

to obtain insight on the effect of electrical conductivity on induced electric field in the brain, two sets of conductivity of brain were considered; (i) the conductivities of white and grey matter were both set to 0.08 S/m and (ii) to 0.16 S/m. The former value is taken from the analysis for NORMAN (Dimbylow 2000, 2008). The latter is rather arbitrary, but well within the uncertainty reported in the literature (Gabriel *et al* 2009). Note that our original electrical conductivities of white and grey matter were 0.06 S/m and 0.1 S/m, respectively (Hirata *et al* 2009). As shown in Table 4, the 99<sup>th</sup> percentile values of the *in-situ* electric field of the brain are almost identical to the original for a uniform  $\sigma$  of 0.08 S/m (middle column), while they were lower by 16-21% for a uniform  $\sigma$  of 0.16 S/m (right column). This tendency coincides with the finding by Dawson *et al* (1998) that the tissue conductivity does not dramatically influence the *in-situ* electric field. This can be also expected from Eq. (1) even though it is applicable only for a sphere.

#### **3.4. Electric Field Induced in Retina and Brain at Threshold Magnetic Flux Density Causing Magnetophosphenes**

The electric fields induced in the brain of all the models and Taro's retina were computed at the nominal threshold exposure causing magnetophosphenes, 8.14 mT at 20 Hz (Lovsund *et al* 1980). The threshold *in-situ* electric field for magnetophosphenes was previously calculated as 53 mV/m for the assumed retinal locus of a homogeneous ellipsoid (IEEE 2002). Even though the threshold in Lovsund *et al* (1980) was based on a non-uniform field exposure, we apply a uniform incident field in this computation. Note that Wake *et al* (1998) computationally showed that current densities in the eye due to uniform exposure and realistic exposures considered in Lovsund *et al* (1980) are comparable to each other.

Figure 4 shows the ratio of the 99<sup>th</sup> percentile values of *in-situ* electric field in the brain and Taro's retina to the IEEE's threshold value of 53 mV/m. As shown, the *in-situ* electric fields in

the brain were 10-80% larger than the threshold, and roughly 50% smaller in Taro's retina for AP and TOP, but about 15% larger for exposure in the LAT direction. The 99<sup>th</sup> percentile *in-situ* electric field in the retina were 61.9 mV/m (LAT), 23.8 mV/m (AP), and 28.7 mV/m (TOP), which are in good agreement with those reported by Dimbylow (2005): 47.5 mV/m (LAT), 23.0 mV/m (AP), and 33.2 mV/m (AP). Induced electric field averaged over the retina (Ilvonen and Laakso, 2009) are also comparable to our results. However, direct comparison cannot be given since incident angles are not the same. Note that a finite element method was used in that paper.

#### **4. Discussion and Summary**

The highest *in-situ* electric fields computed with a voxel spherical model, from beyond the 95<sup>th</sup> percentile to the maximum, revealed obvious differences compared to the analytic solution. This result was similar to a previous study (Dawson *et al* 2001), in which different size models and electrical constants were used. Our computational results suggest that the *in-situ* electric field may vary significantly and nonrepresentatively within the upper 1<sup>st</sup> percentile of voxels. The 99<sup>th</sup> percentile for the computed three-layer model produced good approximations of the analytic solution's maximum at a resolution of 2 mm, with computational errors of less than several percent for the skin and bone and less than 1% for the brain at all resolutions. A similar tendency was observed for anatomically-based models for different resolutions (1 mm and 2 mm). In the voxel models there was little that separated the 98<sup>th</sup> percentile from the 99<sup>th</sup> percentile doses, although the dose curve became steeper after about the 95<sup>th</sup> percentile (Figure 3). However, 99<sup>th</sup> percentile value is used extensively, and was recently adopted by ICNIRP for its 2010 guideline. Therefore, our computed results were presented in the context of this index. The results obtained herein support the approach taken in the ICNIRP guidelines (2010) to approximate the maximum *in-situ* electric field with the 99<sup>th</sup> percentile value computed at a

resolution of 2 mm. It should be noted that the same tendency was observed even when other computational methods were used (Dimbylow 2005, Hirata et al 2010a, Hirata et al 2010b), though the quasi-static FDTD method was used in this study.

The threshold *in-situ* electric field for magnetophosphenes has been derived as 53 mV/m in an adult-sized ellipsoidal model for an empirical exposure threshold of 8.14 mT at 20 Hz (Lovsund et al 1980). However, the corresponding *in-situ* electric field in the central nervous system, until now, was not well investigated in an anatomically-based model. When comparing the 99<sup>th</sup> percentile value in the brain of the anatomically-based model with those derived from an ellipsoidal model described in the IEEE standard, the former was 10-70% larger than the latter. The main reason for the difference between the dose to the brain in the ellipsoidal model with the anatomical model is attributed to the fact that surrounding structures affect induction in the anatomical model, whereas in the ellipsoidal model the brain is an isolated structure. Also, note that the difference of the *in-situ* electric field is influenced by the circumference of the model (See Eq. (1)). On the other hand, in the retina, the actual site of magnetophosphene transduction, the 99<sup>th</sup> percentile induced electric field at the threshold exposure (8.14 mT at 20 Hz), was less than the ellipsoidal model's threshold level (53 mV/m) for the AP and TOP orientations of the exposure field and greater for LAT.

Finally, as can be seen from Table 3, when deriving reference levels or maximum permissible exposures to maintain dose below the basic restriction, the 99<sup>th</sup> percentile value of the *in-situ* electric field serves as a good estimate of a tissue's maximum for a uniform magnetic field exposure.

### **Acknowledgement**

The authors would like to acknowledge Drs. Soichi Watanabe and Tomoaki Nagaoka (NICT)

and Masami Kojima for providing their anatomically based Japanese phantoms (1-mm resolution) and Dr. Kenichi Yamazaki (CRIEPI, Japan) for helpful discussion for preparing this manuscript

.

## References

- Christ A., Kainz W., Hahn E. G., Honegger K., Zefferer M., Neufeld E., Rascher W., Janka R., Bautz W., Chen J., Kiefer B., Schmitt P., Hollenbach H. P., Shen J. X., Oberle M., and Kuster N. 2010 The Virtual Family-Development of anatomical CAD models of two adults and two children for dosimetric simulations *Phys. Med. Biol.* **55** 23-38.
- Dawson T W, Caputa K, Stuchly M A. 1998 Effects of skeletal muscle on human organ dosimetry under 60 Hz uniform magnetic field exposure. *Phys. Med. Biol.* **43** 1059-1074
- Dawson T W, Potter M and Stuchly M A. 2001 Evaluation of modeling accuracy of power frequency field interactions with the human body *ACES Journal* 16 162-72
- De Moerloose J, Dawson T W and Stuchly M A. 1997 Application of FDTD to quasi-static field analysis *Radio. Sci.* **8** 355-75
- Dimbylow P J 1997 FDTD calculations of the whole-body averaged SAR in an anatomically realistic voxel model of the human body from 1MHz to 1GHz *Phys. Med. Biol.* **42** 479-490.
- Dimbylow P J 2000 Current densities in a 2 mm resolution anatomically realistic model of the body induced by low frequency electric fields *Phys. Med. Biol.* **45** 1013-22
- Dimbylow P 2005 Development of the female voxel phantom, NAOMI, and its application to calculations of induced current densities and electric fields from applied low frequency magnetic and electric fields *Phys. Med. Biol.* **50** 1047-70
- Dimbylow P. 2008 Quandaries in the application of the ICNIRP low frequency basic restriction on current density *Phys. Med. Biol.* **53** 133-45
- Gabriel S, Lau R W, and Gabriel C 1996 The dielectric properties of biological tissues: III. Parametric models for the dielectric spectrum of tissues *Phys. Med. Biol.* **41** 2271-293
- Gabriel C, Peyman A, and Grant E H 2009 Electrical conductivity of tissue at frequencies below 1 MHz *Phys. Med. Biol.* **54** 4863-78
- Hirata A, Caputa K, Dawson T W, and Stuchly M 2001 Dosimetry in models of child and adult for

low-frequency electric field *IEEE Trans Biomed Eng* **48** 1007-12

Hirata A, Watanabe S, Fujiwara O, Kojima M, Sasaki K, and Shiozawa T 2007 Temperature elevation in the eye of anatomically based human models for plane-wave exposure *Phys. Med. Biol.* **52** 6389-99

Hirata A, Wake K, Watanabe S, and Taki M 2009 *In-situ* electric field and current density in Japanese male and female models for a uniform magnetic field exposures *Rad. Prot. Dosimetry* **135** 272-5

Hirata A, Yamazaki K, Hamada S, Kamimura Y, Tarao H, Wake K, Suzuki Y, Hayashi N and Fujiwara O 2010a Intercomparison of induced fields in Japanese male model for ELF magnetic field exposures: effect of different computational methods and codes *Rad. Prot. Dosimetry* **138** 237-244

Hirata A, Takano Y, Kamimura Y and Fujiwara O 2010b Effect of averaging volume and algorithm on *in-situ* electric field for uniform electric and magnetic field exposures *Phys. Med. Biol.* **55** N243-252

ICNIRP 1998 Guidelines for limiting exposure to time-varying electric, magnetic, and electromagnetic fields (up to 300 GHz), *Health Phys.* **74**, 494-522

ICNIRP 2010 ICNIRP Statement – Guidelines for limiting exposure to time-varying electric and magnetic field (1 Hz to 100 kHz), *Health Phys.* **99**, 818-836.

IEEE 2002 IEEE Standard for safety levels with respect to human exposure to electromagnetic fields, 0-3 kHz (C95.6).

Iivonen S and Laakso I 2009 Computational estimation of magnetically induced electric fields in a rotating head, *Phys. Med. Biol.* **54**, 341-351.

Lovsund P., Oberg P. A., Nilsson S E, and Reuter T 1980 Magnetophosphenes: A quantitative analysis of thresholds *Med Biol Eng Comput*, **18**, 326-334.

Nagaoka T, Watanabe S, Sakurai K, Kunieda E, Watanabe S, Taki M and Yamanaka Y. 2004 Development of realistic high-resolution whole-body voxel models of Japanese adult males and females of average height and weight, and application of models to radio-frequency electromagnetic-field dosimetry *Phys. Med. Biol.* **49**, 1-15

Nagaoka T, Kunieda E and Watanabe S 2008 Proportion-corrected scaled voxel models for Japanese children and their application to the numerical dosimetry of specific absorption rate for frequencies

from 30 MHz to 3 GHz *Phys. Med. Biol.* **53** 6695-6712

Reilly J P 2003 Mechanisms of electrostimulation: application to electromagnetic field exposure standards at frequencies below 100 kHz. in *The International EMF Dosimetry Handbook*, Chadwick, P. and Gabriel, C. eds. Online: <http://www.emfdosimetry.org>

Stuchly M A and Dawson T W 2000 Interaction of low-frequency electric and magnetic fields with the human body *Proc. IEEE* **88** 643-64

Taflove A and Hagness S 2005 *Computational Electrodynamics: The Finite-Difference Time-Domain Method*: 3rd Ed. Norwood, MA: Artech House

Wake K, Tanaka T, Kawasumi M, and M. Taki. 1998 Induced current density distribution in a human related to magnetophosphenes *Trans. IEE Japan* **118-A** 806-11

Table 1. Height, weight and the number of tissues/organs of anatomically-based models.

	Height [m]	Weight [kg]	Tissue types
TARO	1.73	65	51
HANAKO	1.61	53	51
3-years	0.9	13	51
Duke	1.74	70	84
Ella	1.6	58	84
Thelonious	1.17	17	84
NORMAN	1.76	76	37

Table 2. Maximum, 99<sup>th</sup> percentile, and average values of *in-situ* electric field of three-layer sphere with the resolution of (a) 0.5 mm, (b) 1 mm, and (c) 2 mm.

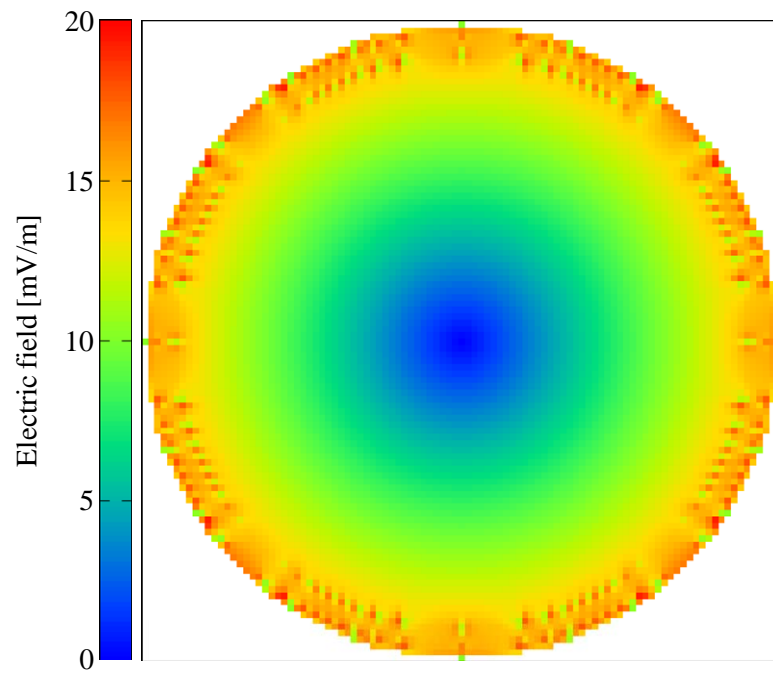
		Max			99 <sup>th</sup> Percentile			Average		
		$E$ [mV/m]		Error [%]	$E$ [mV/m]		Error [%]	$E$ [mV/m]		Error [%]
		Analytic	FDTD		Analytic	FDTD		Analytic	FDTD	
Skin	(a)	15.7	19.9	26.5	15.7	16.7	7.0	12.4	12.2	1.1
	(b)	15.7	19.0	21.1	15.7	17.1	9.2	12.2	12.0	1.6
	(c)	15.7	18.6	18.4	15.6	16.8	7.3	12.2	11.8	3.2
Bone	(a)	15.4	19.5	26.4	15.3	15.7	3.1	11.8	11.8	0.1
	(b)	15.4	20.2	31.2	15.3	16.2	6.5	11.6	11.7	0.4
	(c)	15.4	19.2	24.9	15.2	16.6	9.2	11.6	11.7	0.8
Brain	(a)	14.1	16.4	15.8	13.8	13.8	0.3	8.2	8.2	0.02
	(b)	14.1	16.2	14.8	13.8	13.7	0.6	8.4	8.4	0.005
	(c)	14.1	16.0	12.9	13.8	13.8	0.2	8.3	8.3	0.03

Table 3. Maximum, 99<sup>th</sup> percentile, and average values of *in-situ* electric field [mV/m] of TARO with the resolution of 1 mm and 2 mm for magnetic field exposure. The magnetic flux density and frequency are 1mT and 50Hz.

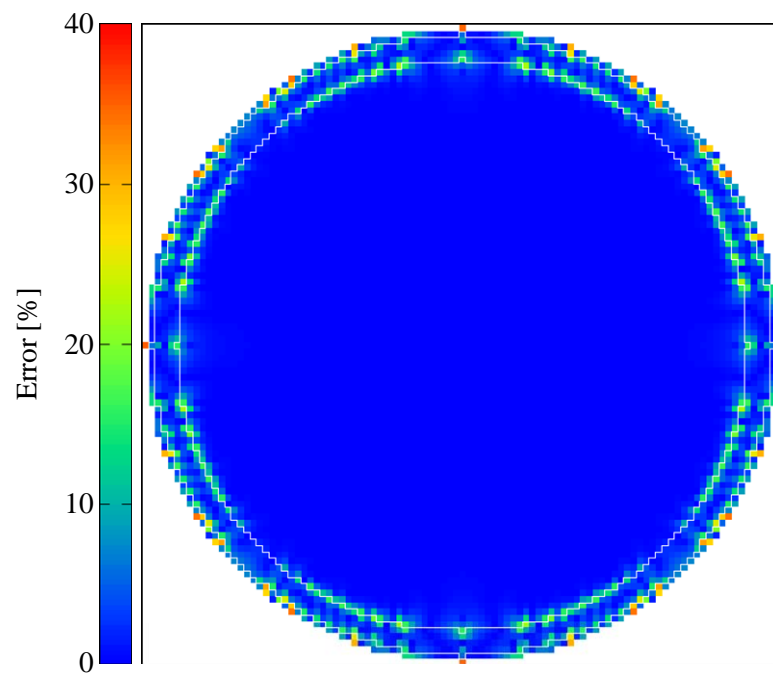
		Max		99 <sup>th</sup> Percentile		Average	
		1mm	2mm	1mm	2mm	1mm	2mm
Brain	LAT	74.1	67.1	27.3	28.5	9.5	9.7
	AP	85.5	69.7	24.6	25.3	8.6	8.8
	TOP	66.2	52.8	20.4	21.4	8.5	8.5
Retina	LAT	39.1	27.5	19.1	19.0	4.9	6.0
	AP	13.1	8.6	6.8	7.3	2.5	2.8
	TOP	12.1	9.4	8.3	8.8	2.6	3.2
Spinal cord	LAT	106	87.8	38.3	38.4	9.0	9.2
	AP	108	85.8	28.9	31.3	4.9	5.1
	TOP	46.0	55.0	21.2	21.7	4.4	4.8
Heart	LAT	66.7	62.6	34.7	34.5	13.0	12.8
	AP	98.9	82.0	37.7	36.1	12.6	12.3
	TOP	52.3	43.8	33.9	32.4	12.8	12.4

Table 4. 99<sup>th</sup> percentile and average values of *in-situ* electric field [mV/m] of TARO with the resolution of 2 mm for a 1-mT, 50-Hz magnetic field exposure, comparing results with original conductivities (left column) for grey (G, 0.08 S/m) and white (W, 0.06 S/m) matter with results for uniform conductivities of 0.08 (middle column) and 0.16 S/m (right column).

		$\sigma$ (S/m)		
		G=0.08/W=0.06 (original)	G=0.08/W=0.08	G=0.16/W=0.16
LAT	L99	28.5	28.3	22.5
	Avg	9.7	9.7	8.5
AP	L99	25.3	25.3	21.0
	Avg	8.8	8.8	8.1
TOP	L99	21.4	21.3	18.0
	Avg	8.5	8.5	8.1

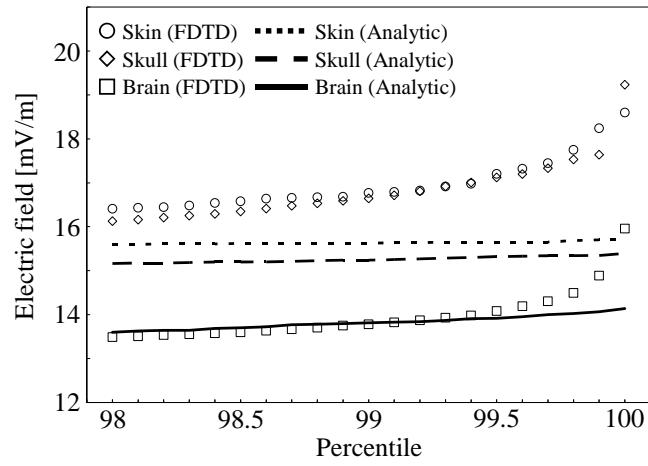


(a)

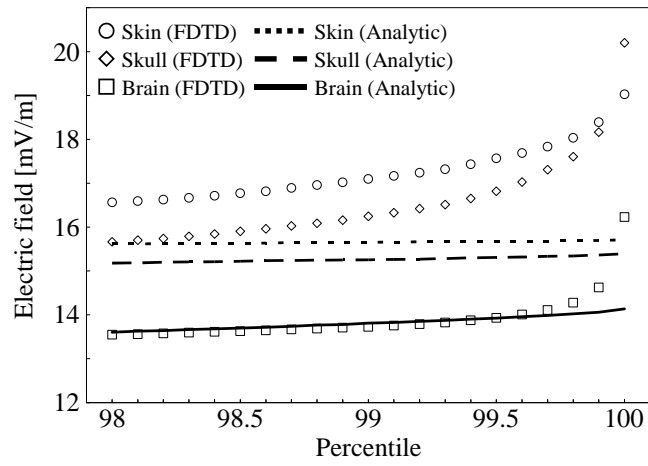


(b)

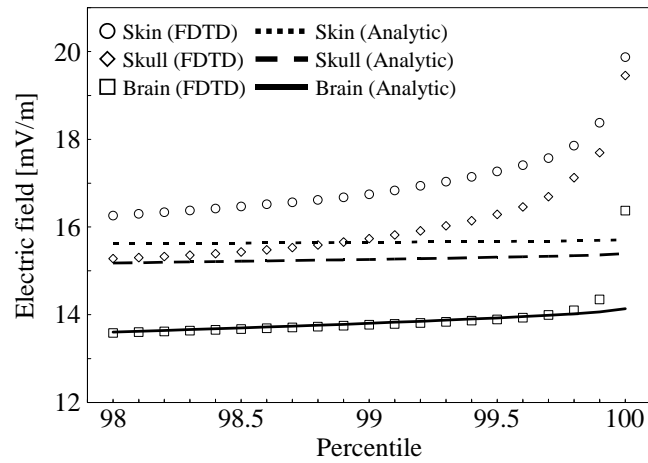
Figure 1: (a) *In-situ* electric field in three-layer sphere computed by quasi-static FDTD method and (b) its error relative to analytic solution. The magnitude and frequency of magnetic flux density are 1 mT and 50 Hz.



(a)



(b)



(c)

Figure 2: Percentile value of *in-situ* electric field in three-layer sphere with the resolution of (a) 2 mm, (b) 1 mm, and (c) 0.5 mm.

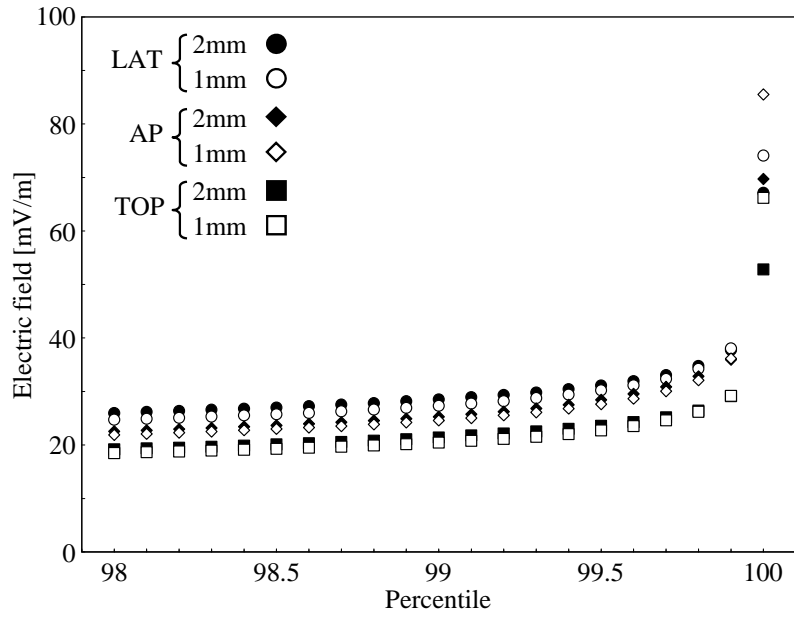


Figure 3: Percentile value of *in-situ* electric field in the brain of TARO with the resolution of 1mm and 2mm. The magnitude and frequency of magnetic flux density is 1mT and 50Hz.

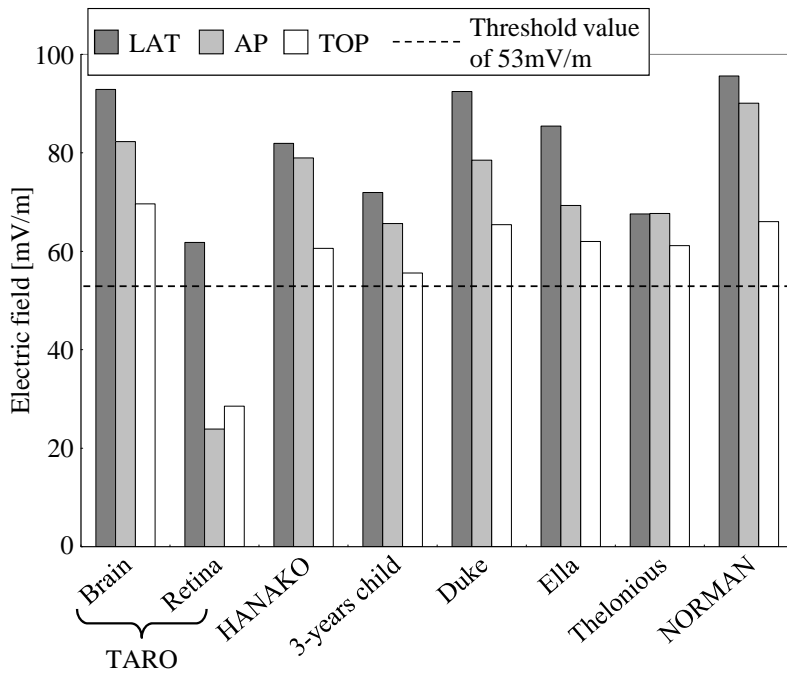


Figure 4: Ratio of computed 99<sup>th</sup> percentile *in-situ* electric field to threshold *in-situ* electric field for magnetophosphenes. Brain is shown for all models with retina added for Taro. The frequency of magnetic flux density is 20 Hz.